Mesoscale variability of phosphorus stocks, hydrological and biological processes in the mixed layer in the Eastern Mediterranean Sea in autumn and during an unusually dense winter phytoplankton bloom

France Van Wambeke, Vincent Taillandier, Xavier Durrieu de Madron, Pascal Conan[4], Mireille Pujo-Pay, Stella Psarra, Sophie Rabouille, Chloé Baumas, Elvira Pulido-Villena

SUPPLEMENTARY INFORMATION:

List of abbreviations
Material and Methods
Table S1 to S6
Figures S1 to S6

List of abbreviations

BP: heterotrophic prokaryotic production
Crypto: cryptophytes-like cells
DCM: deep chlorophyll maximum
DIP: dissolved inorganic phosphorus
DOC: dissolved organic carbon
DON: dissolved organic nitrogen
DOP: dissolved organic phosphorus
EMS: eastern Mediterranean Sea
Hprok: heterotrophic prokaryotes
H500: dynamic topography relative to 500 dbar
L_{DOP}: hydrolysable fraction of DOP
LWCC: liquid waveguide capillary cell
ML: mixed layer
MLD: mixed layer depth
MS: Mediterranean Sea
Nanoeuk: nanophytoeukaryotes
NOx: the sum of nitrate + nitrite
PCA: principal component analysis
Q10: how many times a biological rate or chemical reaction changes when the temperature shifts by 10°C
PDE: phosphodiesterase
Picoeuk: picophytoeukaryotes
PISO : depth of isopycnal 29.05 kg m^{-3}
PME : phosphomonoesterase
PP : primary production
Proc : *Prochlorococcus*
Syn : *Synechococcus*
σ: excess density
Tchla : total chlorophyll a
ZNcline: nitracline depth
ZPcline: phosphacline depth

Material and Methods

Phosphacline and nitracline depths

The phosphacline (nitracline) was defined for each station as the layer with maximum vertical gradient of DIP (NOx) concentration (computed as the highest significant slope of the linear fitting of DIP (NOx) concentration as a function of depth). The set of concentrations selected inside phosphacline (nitracline) included 3 to 9 data points and varied from 38 ± 19 nM to 158 ± 40 nM for DIP and from 1.3 ± 0.8 µM to 3.5 ± 1.4 µM for NOx. The depth of the top of the PCline (NCline) was defined as the intercept of the regression line, which is the highest depth at which DIP (NOx) concentration is zero (Moutin and Prieur, 2012). See example Fig. S1b. In the case of DIP versus depth relationship we used the DIP concentrations determined with the LWCC technique for depleted layers and classical DIP measurements for replete layers (> 0.08 µM). When a 'staircase' effects was seen on the plot showing 2 zones of gradients of concentration with depth, we considered the deepest one to calculate the nitracline and phosphacline depths.

DIP and NOx gradients across isopycnals

'DIP and NOx gradients across isopycnals (∂DIP/$\partial\sigma$ and ∂NOx/$\partial\sigma$) at the nutriclines were calculated as the slope of the linear fitting of the relationship between nutrient concentrations and σ. We identified the maximum gradient of DIP (Nox) across isopycnals (computed as the highest significant slope of the linear fitting of DIP (NOx) concentration as a function of σ (see example Figure S1a). For DIP a second DIP gradient from the surface to the upper boundary of the P-cline (i.e. inside the P-depleted layer, across the ML) was also considered when detectable as suggested in Du et al. (2017) and Pulido-Villena et al. (2021), (i.e. when DIP vs sigma increased linearly). In such cases, the set of concentrations selected varied from 10 ± 4 to 22 ± 8 nM.'

Du, C., Liu, Z., Kao, S.-J., Dai, M. (2017). Diapycnal fluxes of nutrients in an oligotrophic oceanic regime: The South China Sea. Geophys. Res. Lett. 44, 11,510–11,518. https://doi.org/10.1002/2017GL074921

Moutin, T. and Prieur, L. (2012). Influence of anticyclonic eddies on the Biogeochemistry from the Oligotrophic to the Ultraoligotrophic Mediterranean (BOUM cruise), Biogeosciences, 9, 3827–3855, https://doi.org/10.5194/bg-9-3827-2012

Table S1. Medians, first and 3rd percentiles (in brackets) of selected physical and biogeochemical parameters among the different groups of stations according to the PCA results (see Fig. 3, Table 1): group A corresponds to PERLE1 cruise (autumn situation, Ierapetra gyre), groups B to F PERLE 2 cruise (winter/spring situation). * In B group, medians at ST50 in the center of the Ierapetra anticyclone, are indicated in italics.

parameter	units	A	B*	C	D	E	F
Mixed layer depth	m	30	103 *213*	57	50	22	145
		[22-37]	[83-158]	[47-88]	[49-51]	[17-27]	[131-207]
Depth of ispopycnal 29.05	m	282	408 *408*	212	100	88	191
		[270-288]	[401-429]	[193-216]	[86-113]	[40-130]	[95-249]
dynamic height ref 500 dbar	dyn m	-0.238	-0.320 *-0.341*	-0.390	-0.416	-0.416	-0.395
		[-0.263 -0.209]	[-0.331-0.306]	[-0.394 -0.39]	[-0.418 - 0.414]	[-0.422 -0.409]	[-0.398 -0.391]
Temperature	°C	24.9	16.9 *16.6*	15.6	16.1	16.4	15.7
		[24.8-25.8]	[16.6-17.3]	[15.5-15.9]	[16.1-16.2]	[15.3-16.6]	[15.6-16.0]
Salinity	PSU	39.70	39.29 *39.28*	39.04	39.21	39.22	39.19
		[39.68-39.73]	[39.28-39.31]	[38.99-39.16]	[39.21-39.22]	[39.21-39.23]	[39.15-39.25]
depth of nitracline	m	123	211 *210*	89	85	21	90
		[101-139]	[172-225]	[70-109]	[58-93]	[0-46]	[75-139]
depth of phosphacline	m	145	257 *257*	94	103	59	163
		[120-181]	[217-261]	[72-114]	[74-127]	[31-83]	[122-205]
∂NOx/∂σ gradient	mmol kg^{-1}	16	18 *18.9*	34	55	51	28
		[15-17]	[16-19]	[33-42]	[52-60]	[42-58]	[27-28]
∂DIP/∂σ gradient	µmol kg^{-1}	993	800 *799*	1301	2753	2410	1274
		[935-1003]	[634-841]	[1172-1375]	[2670-3038]	[2315-2726]	[1230-1521]
NOx	µM	0.011	0.48 *049*	0.77	0.700	0.29	1.10
		[0.010-0.016]	[0.44-0.50]	[0.40-0.83]	[0.60-0.79]	[0.22-0.40]	[1.09-1.13]
DIP	nM	10.2	8.4 *8.3*	9.9	9.7	9.1	23.3
		[7.9-12.4]	[8.3-9.2]	[9.1-10.7]	[7.8-11.0]	[8.9-9.5]	[21.9-24.2]
DOP	nM	22	50 *63*	49	38	49	70
		[20-34]	[30-66]	[44-53]	[29-42]	[37-55]	[65-73]
L_{DOP}	nM	6.2	11.4 *8.7*	11.1	13.9	13.5	29.4
		[4.0-7.5]	[8.6-14.8]	[7.3-13.6]	[12.4-15.3]	[10.9-16.5]	[11.0-33.7]
DON	µM	5.2	4.5 *4.7*	4.4	4.3	4.6	4.3
		[4.8-5.7]	[4.3-4.8]	[4.2-4.7]	[4.1-4.4]	[4.5-4.7]	[4.2-4.5]
DOC	µM	80	*65 64*	60	60	60	57
		[78-81]	[62-66]	[58-63]	[59-62]	[58-65]	[56-58]
% L_{DOP}	%	23	20	18	33	30	41
		[14-38]	[14-50]	[14-26]	[31-51]	[27-33]	[14-53]
NOx:DIP molar ratio		1.5	55	67	79	32	47
		[1.3-2.3]	[51-59]	[38-75]	[68-87]	[25-46]	[43-54]

Table S2. Medians, first and 3rd percentiles (under brackets) of abundances of microorganisms: *Synechococcus* (Syn), *Prochlorococcus* (proc) picophytoeucaryotes (Picoeuk), nanophytoeucaryotes (Nanoeuk); heterotrophic bacterial abundances (Hprok); BP rates; PME and PDE kinetic characteristics (Vm, Km) as well as cell specific and biomass specific Vm rates among the different groups of stations according to the PCA results (see Fig. 3; Table 1): group A corresponds to PERLE1 cruise (autumn situation, Ierapetra gyre), groups B to F PERLE 2 cruise (winter/spring situation).*Pigments were not available at some stations, see methods.

parameter	units	A	B	C	D	E	F
Tchla*	µg L^{-1}	0.047	0.23	0.26	0.45	0.42	0.23
		[0.043-0.054]	[0.23-0.25]	[0.24-0.26]	[0.36-0.47]	[0.42-0.45]	[023-0.24]
Proc	x 10^3	0.58	1.16	1.95	3.68	3.16	0.89
	cell mL^{-1}	[0.4-0.7]	[0.8-1.2]	[1.6-2.1]	[3.0-5.1]	[3.0-4.1]	[0.82-0.91]
Syn	x 10^3	12	2.0	2	3.8	5.6	0.7
	cell mL^{-1}	[11-13]	[1.7-2.2]	[2.0-2.4]	[3.6-4.6]	[5.2-6.0]	[0.6-0.8]
Picoeuk	cell mL^{-1}	495	76	70	218	205	208
		[407-592]	[60-106]	[63-81]	[195-259]	[174-269]	[62-251]
Nanoeuk	cell mL^{-1}	87	21	22	21	49	15
		[65-97]	[12-27]	[19-27]	[20-24]	[39-52]	[12-16]
Hprok	x10^5	3.3	4.1	3.3	6.7	4.2	3.7
	cells mL^{-1}	[3.0-3.7]	[3.9-4.3]	[3.0-4.3]	[6.5-7.0]	[3.9-5.2]	[3.6-4.0]
BP	ngC L^{-1} h^{-1}	ND	7.4	9.6	28.3	22.8	6.7
			[6.2-12.7]	[8.4-11.2]	[24.5-30.9]	[17.1-27.4]	[6.3-7.2]
Vm PME	nmol MUF-P	2.3	3.8	1.9	5.2	11.1	0.34
	hydr L^{-1} h^{-1}	[1.9-2.6]	[1.5-4.9]	[1.7-3.7]	[4.7-5.9]	[9.3-16.1]	[0.22-0.41]
Vm PDE	nmol bis MUF-P	2.5	7.2	5.5	7.2	18.3	0.20
	hydr L^{-1} h^{-1}	[1.7-4.2]	[3.4-8.5]	[3.2-7.3]	[6.9-7.4]	[14.4-21.1]	[0.16-0.42]
Km PME	µM	0.063	0.14	0.10	0.20	0.22	0.14
		[0.059-0.068]	[0.11-0.19]	[0.093-0.12]	[0.17-0.23]	[0.19-0.27]	[0.12-0.19]
Km PDE	µM	2.6	5.8	4.1	6.30	6.6	1.3
		[2.1-4.3]	[3.9-6.8]	[3.2-5.1]	[5.9-6.5]	[6.5-6.8]	[1.0-1.5]
TT PME	days	1.16	1.84	2.16	1.74	0.82	19.9
		[1.05-1.31]	[1.61-2.74]	[1.46-2.28]	[1.21-2.24]	[0.73-0.91]	[15.5-27.9]
TT PDE	days	45	36	25	36	15	230
		[39-52]	[32-44]	[24-41]	[35-42]	[14-19]	[162-326]
cell specific	x10^{-18} mol	7	10	6	7	23	1.0
Vm PME	hydr $cell^{-1}$ h^{-1}	[5-8]	[4-12]	[4-10]	[6-9]	[20-29]	[0.5-1.2]
cell specific	x10^{-18} mol	8	17	14	11	36	0.7
Vm PDE	hydr $cell^{-1}$ h^{-1}	[5-13]	[8-20]	[10-27]	[10-11]	[33-36]	[0.4-1.1]
biomass sp							
	nmol hydr	0.32	0.16	0.13	0.17	0.45	0.017
Vm PME	[µgC]$^{-1}$ h^{-1}	[0.29-0.36]	[0.09-0.19]	[0.09-0.18]	[0.14-0.21]	[0.37-0.59]	[0.013-0.024]
biomass sp	nmol hydr	0.32	0.35	0.39	0.30	0.74	0.013
Vm PDE	[µgC]$^{-1}$ h^{-1}	[0.23-0.48]	[0.25-0.43]	[0.28-0.66]	[0.26-0.33]	[0.61-0.88]	[0.010-0.027]

Table S3. DIP ($\partial DIP/\partial\sigma$) and NOx ($\partial NOx/\partial\sigma$) gradients accross isopycnals, values ± standard deviation and corresponding significance of the regressions (p). Gradients were estimated from nitracline for NOx and from phosphacline for DIP. In some cases, it was also possible to determine a secondary DIP gradient inside P depleted layer (across the ML), when detectable (see supplementary information - material and methods for details); nd: not determined, in italics $p > 0.05$.

			from nitracline		from phosphacline		inside P-depleted layer	
			mmol kg^{-1}		µmol kg^{-1}		µmol kg^{-1}	
cruise	group	st	∂NOx/∂σ	p	∂DIP/∂σ	p	∂DIP/∂σ	p
PERLE1	A	2	12.1 ± 0.9	< 0.01	887 ± 161	0.03	*2.5 ± 1.3*	*0.16*
PERLE1	A	5	15.8 ± 0.4	< 0.01	994 ± 53	0.03	3.8 ± 1.1	0.02
PERLE1	A	12	15.3 ± 0.8	< 0.01	766 ± 73	< 0.01	*9.0 ± 5.9*	*0.37*
PERLE1	A	15	16.1 ± 0.8	< 0.01	973 ± 110	0.013	6.2 ± 1.4	0.04
PERLE1	A*	16	15.0 ± 1.4	< 0.01	1011 ± 58	< 0.01	2.8 ± 0.8	0.04
PERLE1	A	19	16.2 ± 0.4	< 0.01	993 ± 37	< 0.01	*5.8 ± 3.6*	*0.35*
PERLE1	A	20	18.3 ± 0.9	< 0.01	1187 ± 70	< 0.01	nd	
PERLE1	A	23	15.7 ± 1.1	< 0.01	919 ± 90	< 0.01	3.6 ± 0.8	0.02
PERLE1	A	25	17.4 ± 0.6	< 0.01	995 ± 105	0.011	3.0 ± 0.8	0.02
PERLE1	A	27	15.5 ± 1.7	< 0.01	1334 ± 77	< 0.01	nd	
PERLE1	A	30	17.4 ± 1.2	< 0.01	952 ± 89	< 0.01	10.3 ± 1.5	0.09
PERLE2	F	1	26.5 ± 4.0	0.02	1186 ± 83	< 0.01	nd	
PERLE2	F	13	28.5 ± 1.4	< 0.01	*1768 ± 198*	*0.07*	385 ± 84	0.02
PERLE2	F	15	28.3 ± 1.4	< 0.01	1275 ± 68	0.03	nd	
PERLE2	C	21	42.3 ± 3.1	< 0.01	3406 ± 770	0.05	102 ± 7	0.04
PERLE2	C	26	32.7 ± 1.4	< 0.01	1301 ± 21	< 0.01	nd	
PERLE2	C	35	*34.5 ± 2.8*	*0.05*	1375 ± 83	0.04	nd	
PERLE2	C	44	18.4 ± 0.8	< 0.01	1172 ± 51	< 0.01	nd	
PERLE2	B	50	18.9 ± 0.6	< 0.01	800 ± 25	0.020	nd	
PERLE2	D*	58	50.0 ± 0.3	< 0.01	2754 ± 45	0.010	nd	
PERLE2	E	68	38.1 ± 5.6	< 0.02	*2370 ± 525*	*0.139*	*310 ± 127*	*0.14*
PERLE2	C	75	44.3 ± 3.3	< 0.03	*700 ± 219*	*0.085*	nd	
PERLE2	E	80	59.7 ± 4.1	< 0.01	3549 ± 301	< 0.01	nd	
PERLE2	E	90	57.5 ± 7.7	0.02	*2451 ± 305*	*0.079*	*97 ± 62*	*0.36*
PERLE2	E	94	43.8 ± 1.4	0.02	*2150 ± 185*	*0.055*	nd	
PERLE2	B	104	*19.2 ± 4.0*	*0.13*	*883 ± 206*	*0.146*	429 ± 133	0.05
PERLE2	B	108	13.3 ± 1.0	0.05	*469 ± 92*	*0.123*	*100 ± 21*	*0.13*
PERLE2	D	111	55.0 ± 1.5	< 0.01	3322 ± 124	0.024	nd	
PERLE2	D	116	64.5 ± 1.2	0.01	*2587 ± 458*	*0.112*	268 ± 60	0.02

Table S4. Correlation coefficients (Pearson) between hydrological and biotic variables. Abiotic variables are mixed layer depth (MLD), depth of isopycnal 29.05 kg m^{-3} (PISO), dynamic topography relative to 500 dbars (H500), DIP gradient across isopycnals (∂DIP/$\partial\sigma$), phosphacline depth, NOx gradient across isopycals (∂NOx/$\partial\sigma$) and nitracline depth. Biotic variables are medians within the mixed layer for nutrient concentrations (DIP, NOx, Si), dissolved organic matter (L_{DOP}, DOP, DOC), Total chlorophyll a (Tchla) abundances of cells (*Prochlorococcus* (Proc), *Synechococcus* (Syn), picophytoeukaryotes (Pico-euk), nanophytoeukaryotes (Nano-euk), Cryptophytes-like cells (Crypto), heterotrophic prokaryotes (hprok) with high and low nucleic acid content (HNA, LNA, respectively), and kinetic parameters of phosphomonoesterase (Km PME, Vm PME) and phosphodiesterase (Vm PDE, Km PDE). n = 27 stations, no data = insignificant correlations ($p > 0.05$), in red positive correlations, in bold r > 0.7 or < -0.7.

	DIP	NOx	Si	L_{DOP}	DOP	DOC	Tchl a	Proc	Syn	Pico-euk	Nano-euk	Crypto	LNA	HNA	Hprok	Vm PME	Km PME	Vm PDE	Km PDE
MLD	0.51	**0.70**			0.57	-0.42			-0.50	-0.39	-0.46					-0.40		-0.40	-0.43
H500		-0.62	**-0.75**	-0.49	-0.67	**0.85**	-0.73	-0.57	**0.76**	**0.71**	**0.78**		-0.55		-0.52	-0.39	-0.69	-0.40	
PISO			-0.66		-0.41	0.48	-0.49	-0.53				-0.54	-0.51		-0.53	-0.48	-0.50	-0.44	
∂DIP/∂σ			**0.72**			-0.46	0.67	0.67				0.62	0.49	0.44	0.67	0.61	0.65	0.52	
ZPcline			-0.40					-0.54				-0.46			-0.39	-0.47		-0.46	
∂NOx/∂σ			**0.74**			-0.62	**0.73**	0.63	-0.43	-0.38	-0.44	0.60	0.67		**0.71**	0.67	**0.73**	0.64	
ZNcline			-0.52				-0.42	-0.56				-0.44	-0.43		-0.42	-0.49		-0.46	

Table S5. Correlation coefficients (Pearson) between hydrological variables and pigments concentrations or ratios, taken at the median values within the mixed layer. Pigment data were 19' butanoyloxyfucoxanthin (19'BF), fucoxanthin (fuco), 19' hexanoyloxyfucoxanthin (19'HF), zeaxanthin (zea), totalchlorophyll b (Tchlb) and total chlorophylla (Tchla). Correlation with some pigment's ratios were also determined: Fuco:Tchla, Chlb:Tchla and 19'BF:Tchla. n = 17 stations, no data = insignificant correlations ($p > 0.05$), in red positive correlations, in blue negative correlations, in bold $r > 0.7$ or < -0.7

	19'BF	Fuco	19'HF	Zea	Tchlb	TChla	Fuco :Tchla	chl b :Tchla	19'BF :Tchla
MLD	0.49						0.49	0.63	**0.70**
H500	**-0.81**	**-0.83**	**-0.78**	**-0.75**	**-0.76**	**-0.76**	-0.51	-0.64	
PISO		**-0.79**	-0.54	-0.67	**-0.80**	-0.70		-0.62	
∂DIP/∂σ		0.66	0.69	**0.82**	**0.71**	**0.79**			
ZPcline		-0.51		-0.68		-0.56			0.57
∂NOx/∂σ		**0.69**	**0.73**	**0.89**	**0.73**	**0.82**			
ZNcline		-0.65	-0.50	-0.68	-0.60	-0.64			0.48

Table S6. Correlation coefficients (Pearson) between hydrological variables and biotic variables taken as integrated stocks. Integrated (0-200 m) abundances of *Prochlorococcus* (I Proc), *Synechococcus* (I Syn), picophytoeukaryotes (I Picoeuk), nanophytoeukaryotes (I Nanoeuk), Cryptophytes-like cells (I Crypto), heterotrophic prokaryotes (I hprok)). Integrated DIP, L_{DOP}, NOx (0-200m) and total chlorophyll a (I Tcha, 0-250 m). n = 27 stations, no data = insignificant correlations ($p > 0.05$), in red positive correlations, in blue negative correlations, in bold $r > 0.7$ or < -0.7.

	I Proc	I Syn	I Pico	I Nano	I Crypto	I Hprok	I DIP	I L_{DOP}	I DOP	I NOx	I Tchla
MLD	-0.41					0.40			0.63		0.59
H500	**0.75**	**0.91**	**0.75**	**0.87**			-0.62	-0.49	-0.60	**-0.78**	-0.64
PISO		0.40			-0.47		**-0.76**			**-0.77**	
∂DIP/∂σ	-0.40	-0.43		-0.42	0.47		**0.71**			**0.76**	
Z Pcline							**-0.74**			**-0.72**	
∂NOx/∂σ	-0.57	-0.58	-0.41	-0.57	0.54	0.51	**0.72**			**0.80**	0.46
ZNcline					-0.39		**-0.76**			**-0.76**	

Supplement Figure captions

Fig. S1 Computation of $\partial DIP/\partial \sigma$ (a) and ZPcline depth (a) at ST26 of PERLE2 cruise.

Fig S2 Vertical profile of NOx versus depth at ST1, showing to possible modes of estimation of ZNcline

Fig. S3. Vertical distributions (0-300 m) of a, d, g: density excess (σ, dotted lines) and fluorescence (continuous lines); b,e,h: dissolved inorganic phosphorus (DIP); and c,f,i: phosphomonoesterase and phosphodiesterase maximum rates (Vm PME, Vm PDE) for A (a, b, c), B (d,e,f) and C (g, h, i) groups. Groups are organized according the principal component analysis results: Group A clusters stations of the autumn cruise in Ierapetra Gyre, group B stations of the winter cruise more anticyclonic, group C stations of the winter cruise being not clearly under mesoscale influence.

Fig. S4. Vertical distributions (0-300 m) of a, d, g: density excess (σ, dotted lines) and fluorescence (continuous lines); b, e, h: dissolved inorganic phosphorus (DIP); and c, f, i: phosphomonoesterase and phosphodiesterase maximum rates (Vm PME, Vm PDE), for D (a, b, c), E (d,e,f) and F (g, h, i) groups. Groups are organized according the principal component analysis results. Group D and E clusters stations of the winter cruise influenced by the cyclonic Rhode gyre, group F clusters stations of the Cretan sea in the beginning of the cruise.

Fig. S5. Vertical profiles of primary production (PP, in mg C m^{-3} d^{-1}, black upper scale), heterotrophic prokaryotic production (BP, in mg C m^{-3} d^{-1}, red upper scale) and chlorophyll derived from fluorescence profiles (Tchl, µg L^{-1}, lower scale) at the ST15, 35, 75, 83, 90, 116 during the winter cruise (PERLE2)

Fig. S6. Vertical profiles of primary production (PP, in mg C m^{-3} d^{-1}, upper scale) and total chlorophyll a derived from fluorescence profiles (Tchl, µg L^{-1}, lower scale) at the ST3, 14, 24 and 26 during the autumn cruise (PERLE1)

Fig. S7. Box plots distribution of some pigments to Tchla ratios calculated for: fucoxanthin (fuco:Tchla), peridinin (peri:Tchla), zeaxanthine (zea:Tchla), divinyl-chlorophyll a (dv-chla:Tchla), chlorophyll b (chlb:Tchla), 19'butanoylfucoxanthin (19'BF:Tchla), alloxanthin (allo:Tchla) and degradation index. Group A gathers stations of the autumn cruise and, groups B to F gather stations of the winter cruise.

Fig. S8. Time series of potential density anomaly values between 20 m and 250 m, and chlorophyll fluorescence at 50 m and 100 m from Nov 2018 to June 2019 at the E1-M3A site in the Cretan Sea (35°47.16' N, 24°55.19' E, 1440 m depth). The shaded area shows the period of PERLE 2 cruise.

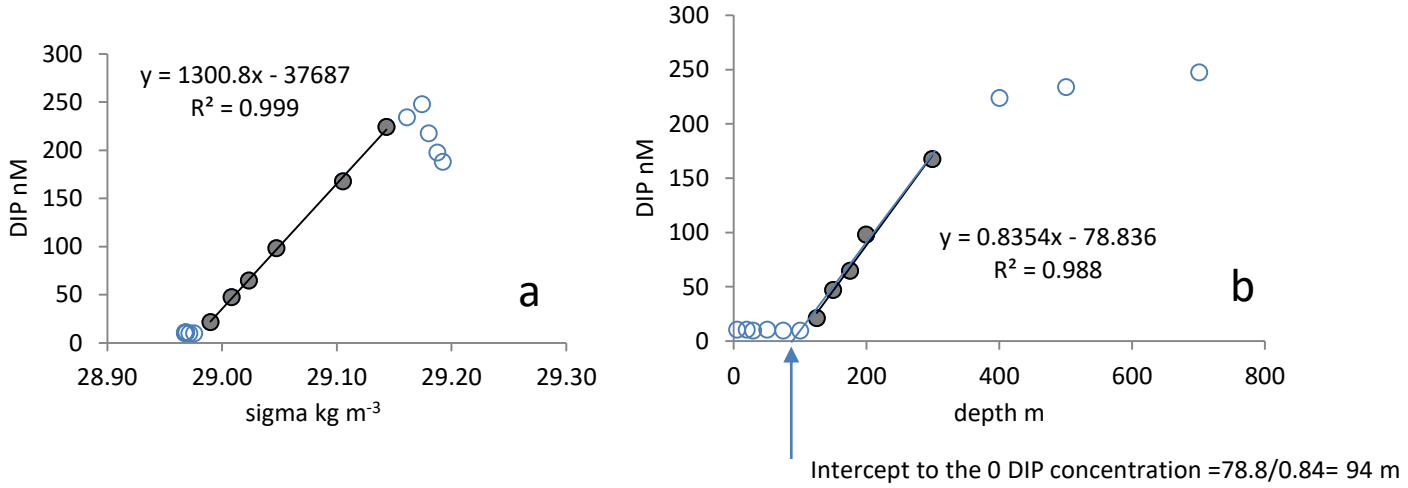
y = 1300.8x - 37687
R² = 0.999
DIP nM
sigma kg m-3
a
y = 0.8354x - 78.836
R² = 0.988
DIP nM
depth m
b
Intercept to the 0 DIP concentration =78.8/0.84= 94 m

Fig. S1

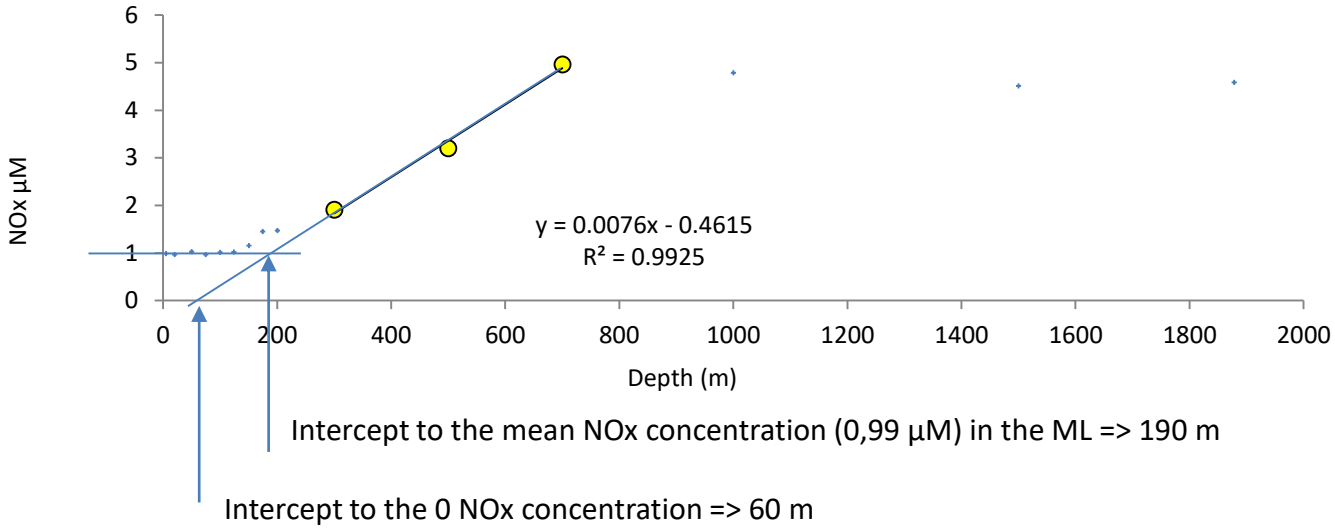
NOx µM
6
5
4
3
2
1
0
0
200
400
600
800
1000
1200
1400
1600
1800
2000
Depth (m)
y = 0.0076x - 0.4615
R² = 0.9925
Intercept to the mean NOx concentration (0,99 µM) in the ML => 190 m
Intercept to the 0 NOx concentration => 60 m

Fig. S2

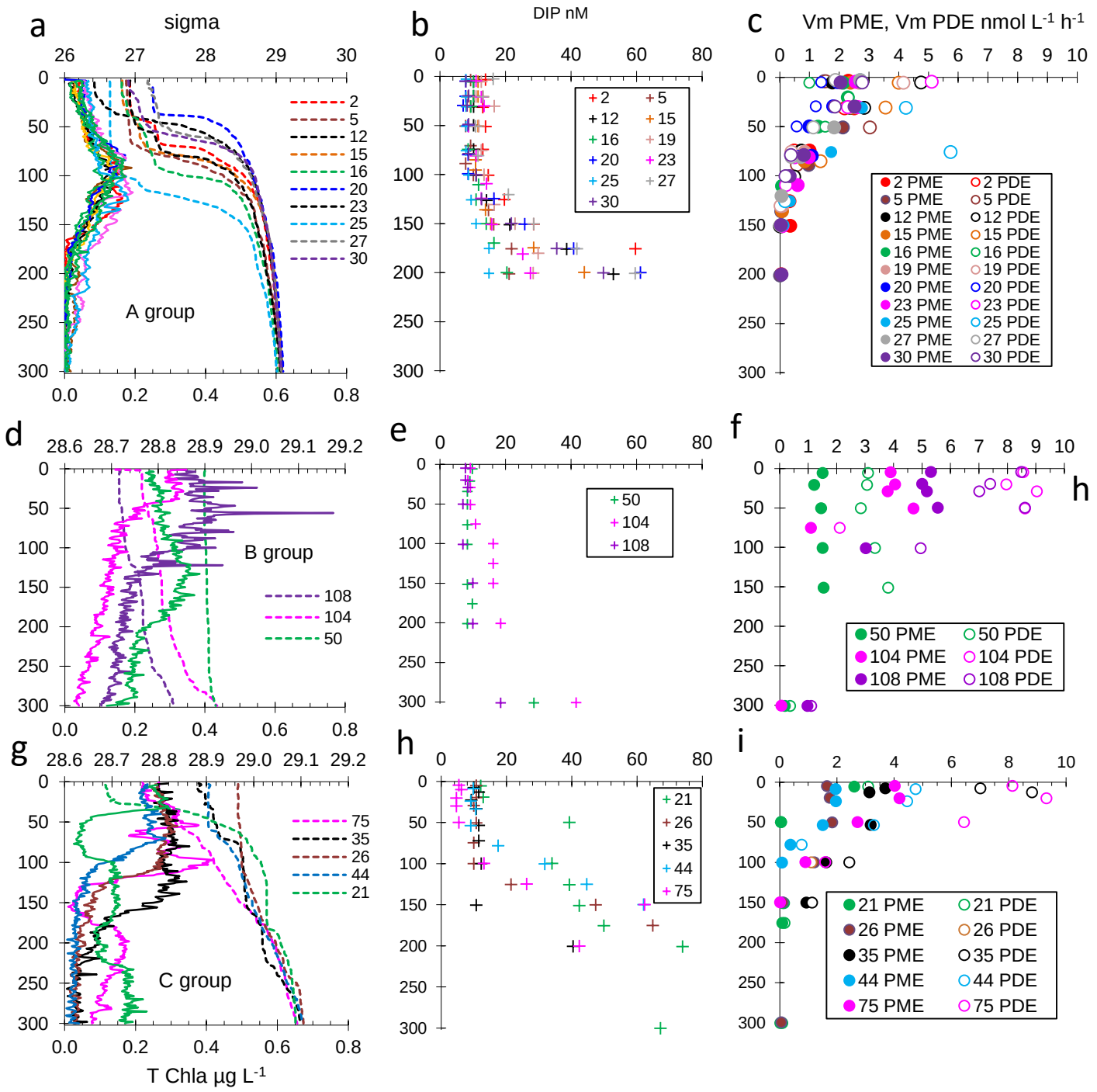
a
sigma
A group
2
5
12
15
16
20
23
25
27
30
b
DIP nM
c
Vm PME, Vm PDE nmol L-1 h-1
2 PME
2 PDE
5 PME
5 PDE
12 PME
12 PDE
15 PME
15 PDE
16 PME
16 PDE
19 PME
19 PDE
20 PME
20 PDE
23 PME
23 PDE
25 PME
25 PDE
27 PME
27 PDE
30 PME
30 PDE
d
B group
108
104
50
e
f
h
50 PME
50 PDE
104 PME
104 PDE
108 PME
108 PDE
g
C group
75
35
26
44
21
T Chla µg L-1
h
i
21 PME
21 PDE
26 PME
26 PDE
35 PME
35 PDE
44 PME
44 PDE
75 PME
75 PDE

Fig. S3

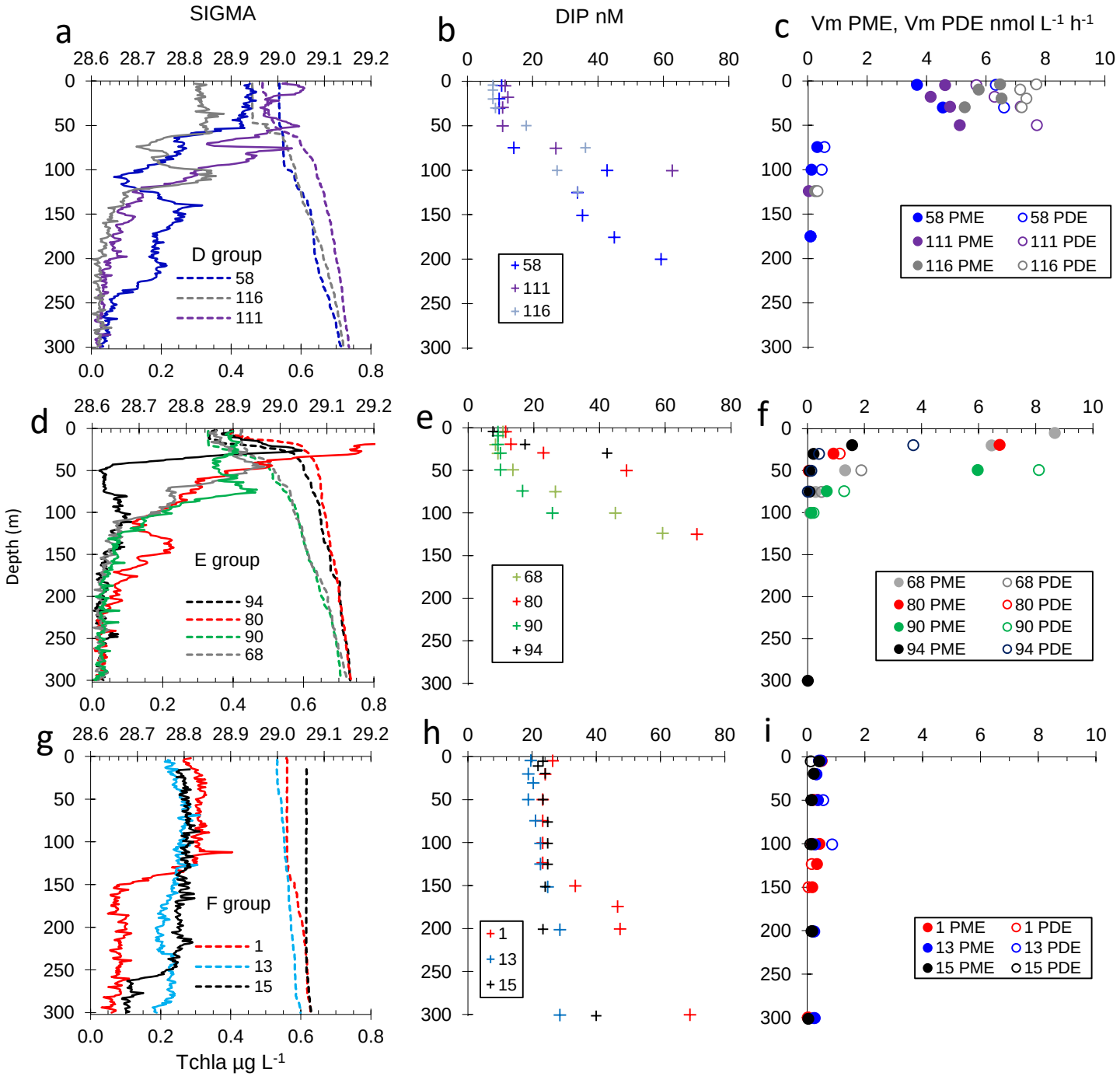
a
SIGMA
28.6 28.7 28.8 28.9 29.0 29.1 29.2
0 50 100 150 200 250 300
0.0 0.2 0.4 0.6 0.8
D group
58
116
111
b
DIP nM
0 20 40 60 80
58
111
116
c
Vm PME, Vm PDE nmol L-1 h-1
0 2 4 6 8 10
58 PME
58 PDE
111 PME
111 PDE
116 PME
116 PDE
d
E group
94
80
90
68
e
68
80
90
94
f
68 PME
68 PDE
80 PME
80 PDE
90 PME
90 PDE
94 PME
94 PDE
Depth (m)
g
F group
1
13
15
Tchla µg L-1
h
1
13
15
i
1 PME
1 PDE
13 PME
13 PDE
15 PME
15 PDE

Fig. S4

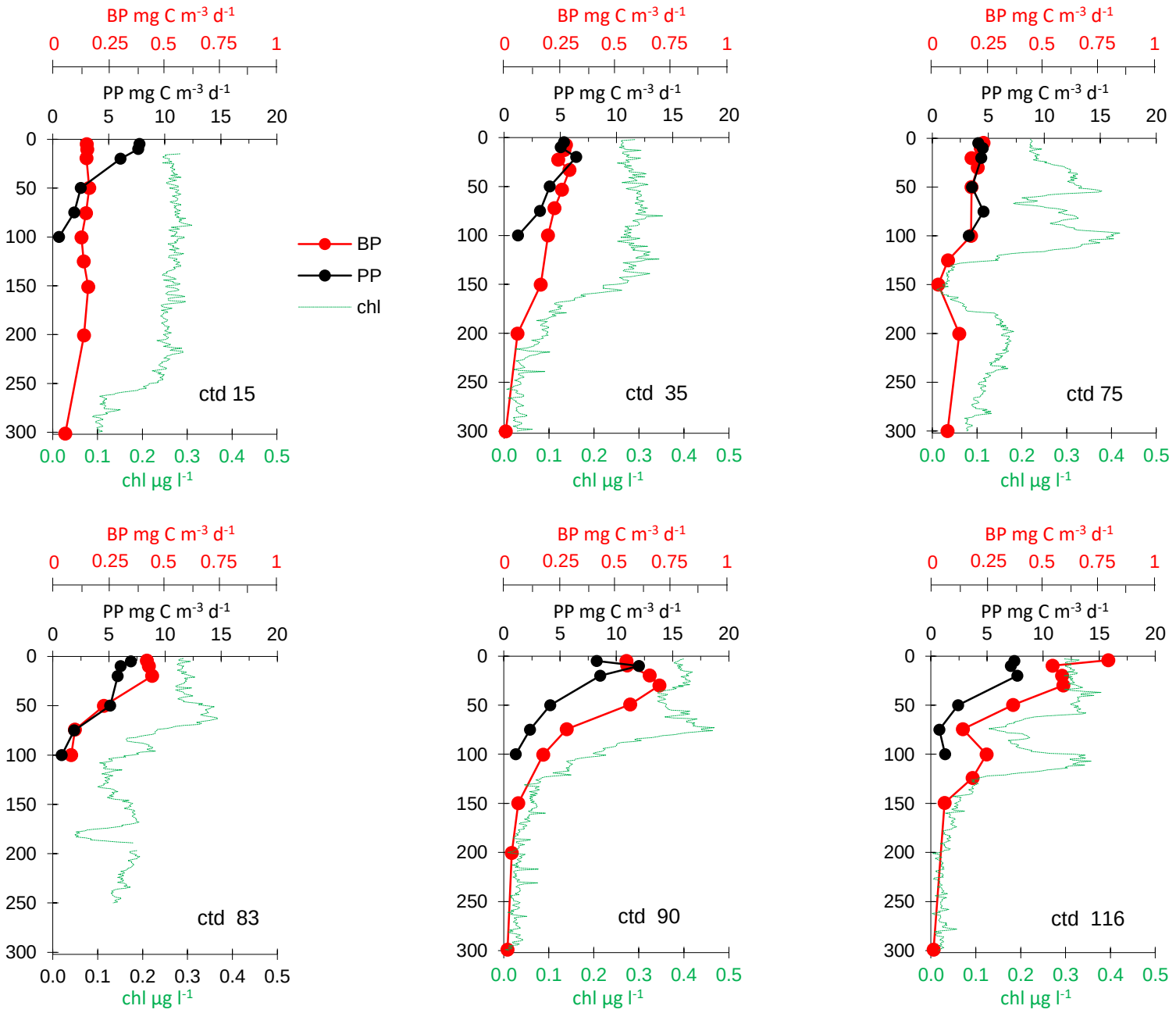
BP mg C m-3 d-1
0 0.25 0.5 0.75 1
PP mg C m-3 d-1
0 5 10 15 20
0 50 100 150 200 250 300
BP
PP
chl
ctd 15
ctd 35
ctd 75
ctd 83
ctd 90
ctd 116
0.0 0.1 0.2 0.3 0.4 0.5
chl µg l-1

Fig. S5

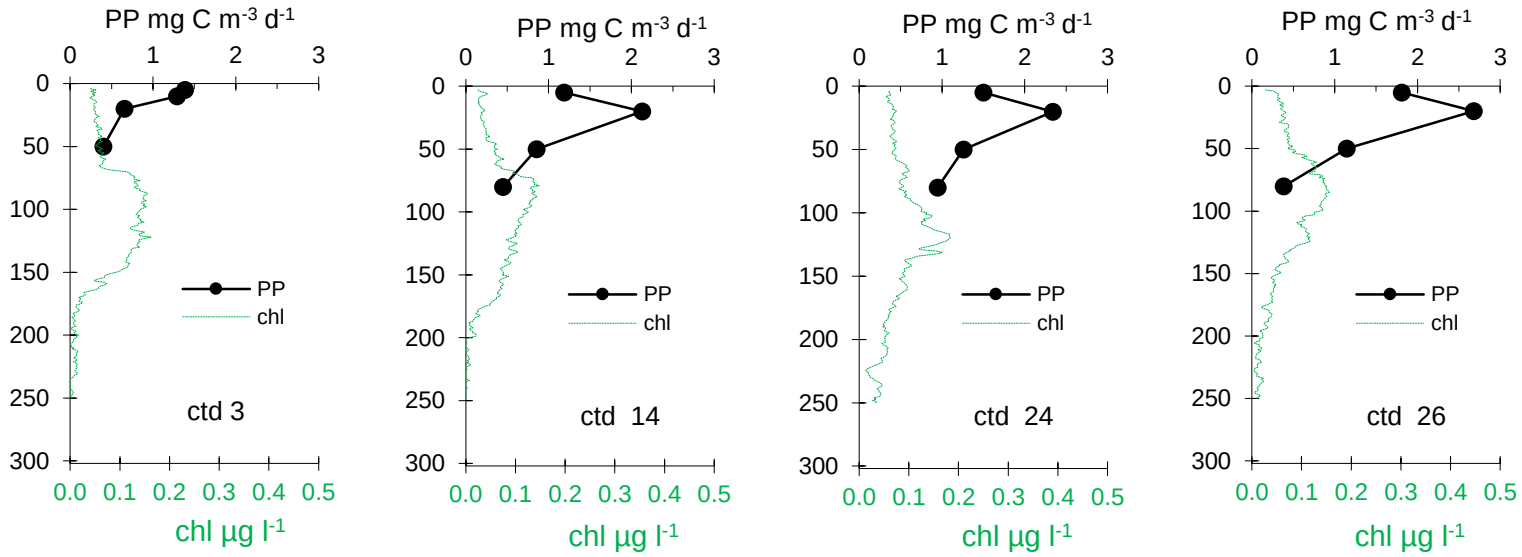
PP mg C m-3 d-1
0 1 2 3
0 50 100 150 200 250 300
PP
chl
ctd 3
0.0 0.1 0.2 0.3 0.4 0.5
chl µg l-1
PP mg C m-3 d-1
0 1 2 3
0 50 100 150 200 250 300
PP
chl
ctd 14
0.0 0.1 0.2 0.3 0.4 0.5
chl µg l-1
PP mg C m-3 d-1
0 1 2 3
0 50 100 150 200 250 300
PP
chl
ctd 24
0.0 0.1 0.2 0.3 0.4 0.5
chl µg l-1
PP mg C m-3 d-1
0 1 2 3
0 50 100 150 200 250 300
PP
chl
ctd 26
0.0 0.1 0.2 0.3 0.4 0.5
chl µg l-1

Fig. S6

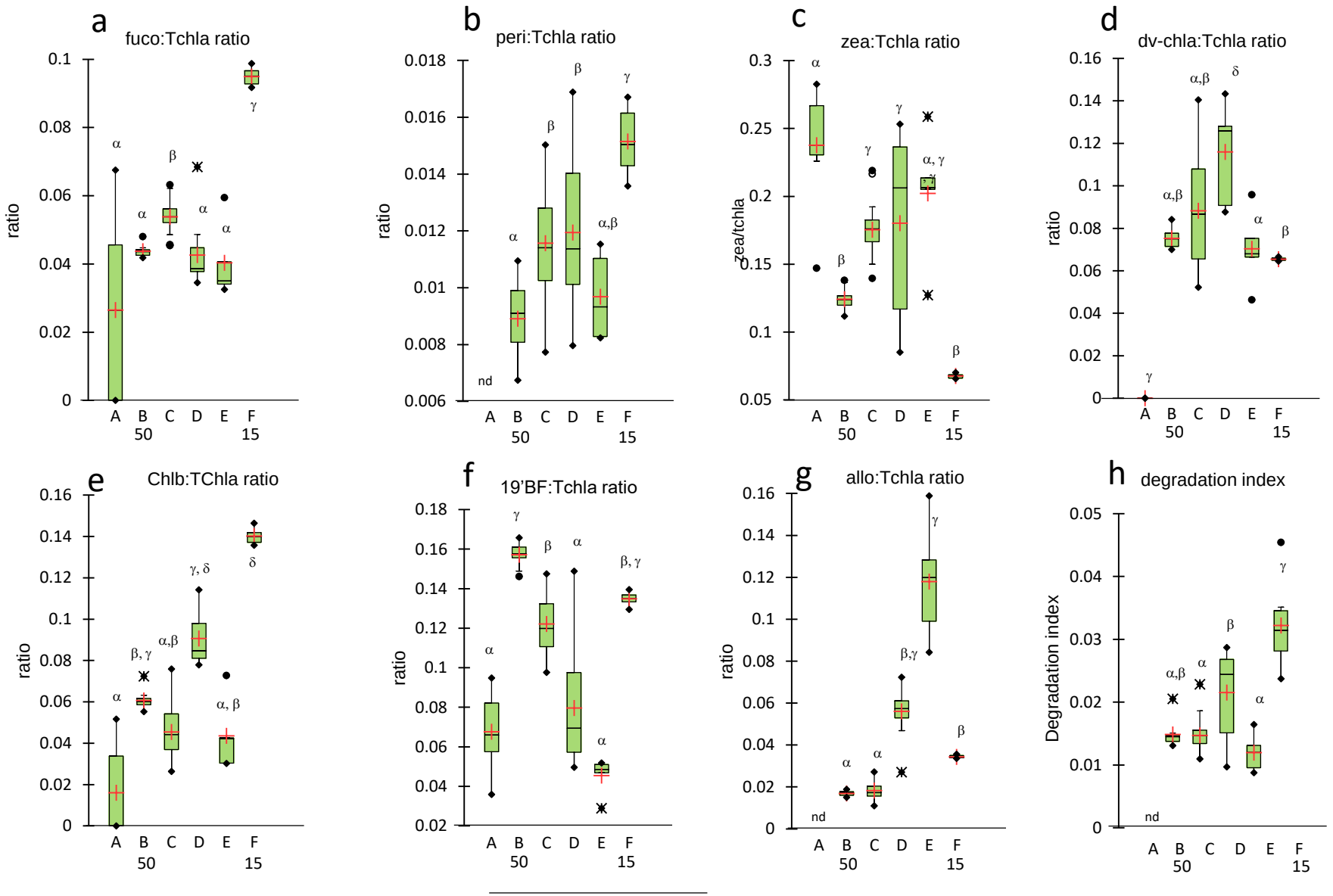
a
fuco:Tchla ratio
ratio
b
peri:Tchla ratio
ratio
nd
c
zea:Tchla ratio
zea/tchla
d
dv-chla:Tchla ratio
ratio
e
Chlb:TChla ratio
ratio
f
19'BF:Tchla ratio
ratio
g
allo:Tchla ratio
ratio
nd
h
degradation index
Degradation index
nd
A B C D E F
50 15

Fig. S7

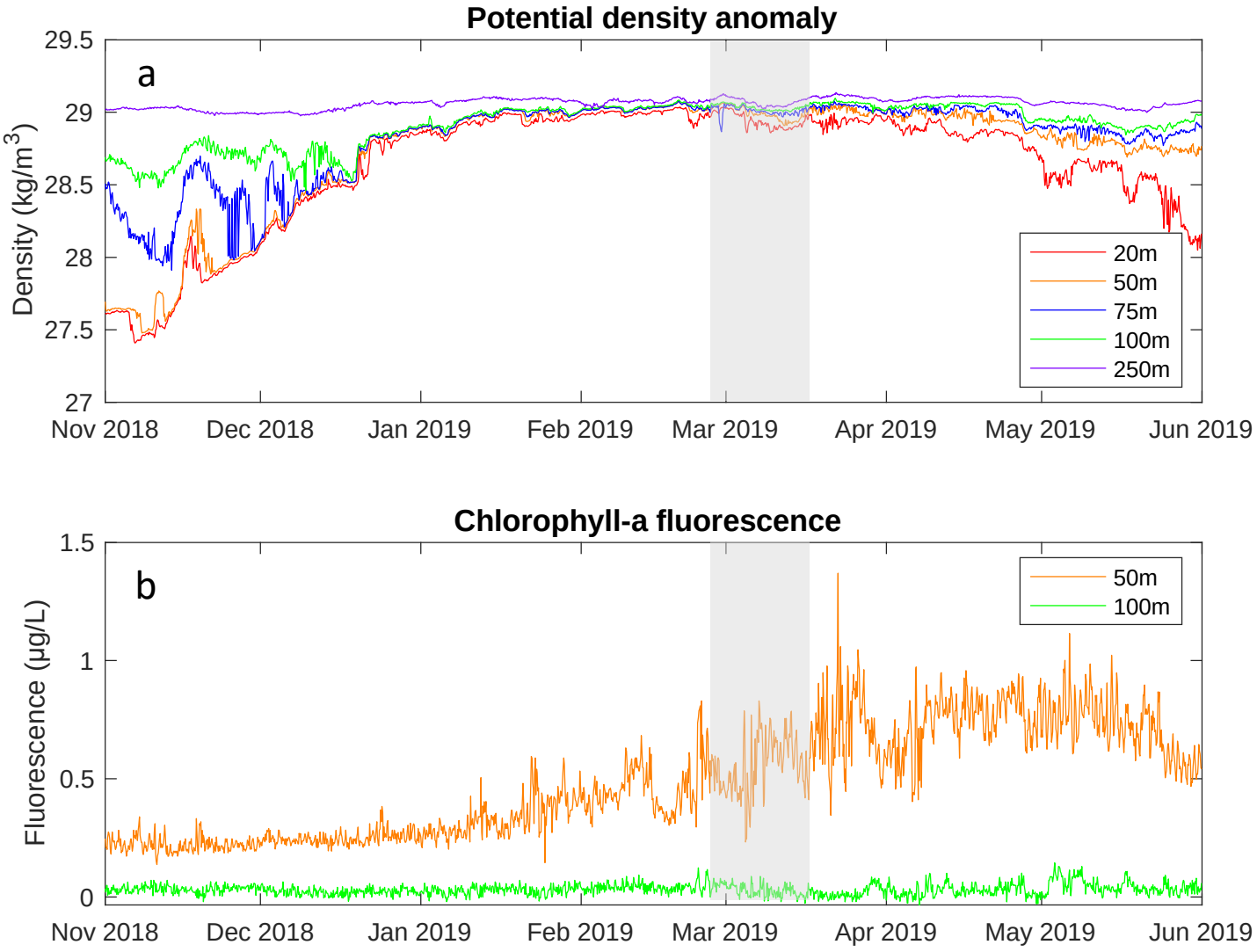
Potential density anomaly
a
Density (kg/m3)
29.5
29
28.5
28
27.5
27
20m
50m
75m
100m
250m
Nov 2018
Dec 2018
Jan 2019
Feb 2019
Mar 2019
Apr 2019
May 2019
Jun 2019
Chlorophyll-a fluorescence
b
Fluorescence (µg/L)
1.5
1
0.5
0
50m
100m
Nov 2018
Dec 2018
Jan 2019
Feb 2019
Mar 2019
Apr 2019
May 2019
Jun 2019

Fig. S8